



# COMPARISON OF DEGRADATION OF METHYLENE BLUE DYE BY ZnO, N DOPED ZnO AND IRON ORE REJECTS

Vrinda Borker<sup>[a]</sup>, Rajashri Karmali<sup>[b]</sup> and Koyar Rane<sup>[c]</sup>

**Keywords:** dye degradation; zinc oxide; N-doped ZnO; iron ore reject; methylene blue

Textile effluent containing unused dye when released in surroundings pollutes water bodies. It requires processing before disposal. Iron ore reject created during mining creates environmental pollution but contains minerals of technological importance. It has ~30-50 % iron in the form of  $\gamma$ -Fe<sub>2</sub>O<sub>3</sub>,  $\alpha$ -Fe<sub>2</sub>O<sub>3</sub> and Fe<sub>3</sub>O<sub>4</sub> is wasted if thrown in fields, so can be used to degrade organic dyes. Mineralization of methylene blue, MB a model dye is carried out using photocatalyst either iron ore reject, synthesized ZnO or ZnO<sub>1-x</sub>N<sub>x</sub> and the results are compared. ZnO is synthesised from oxalate and nitrogen doped ZnO from hydrazinated oxalate precursors. FTIR study of zinc complexes indicates formation of precursors and XRD of decomposed complexes reveal formation of zinc oxide with wurtzite structure. The presence of nitrogen in ZnO<sub>1-x</sub>N<sub>x</sub> is confirmed by chemical estimation and XPS studies. SEM reveals the particle size of ZnO<sub>1-x</sub>N<sub>x</sub> ~69 nm and ZnO ~0.5-1  $\mu$ m. ZnO<sub>1-x</sub>N<sub>x</sub> absorbs in the visible region and ZnO in UV region. Band gap energy calculated using Diffuse reflectance Spectrum is 2.48 eV for the former, 3.19eV for the later and 2.38 eV for ore reject. Mineralizing property of ore reject, ZnO and ZnO<sub>1-x</sub>N<sub>x</sub> are compared by electrons spray ionisation mass spectrometry study (ESI-MS) of degradation products, COD measurement and CO<sub>2</sub>, NO<sub>3</sub><sup>-</sup> and SO<sub>4</sub><sup>2-</sup> estimation. Reusability study, kinetic study of degradation of MB dye using photocatalysts and ESI-MS study of degraded products of MB reveal better efficacy of iron ore rejects amongst three. Thus efficiency of iron ore reject > ZnO<sub>1-x</sub>N<sub>x</sub> > ZnO as photocatalyst.

\* Corresponding Author

Fax: +9108322462315,

Email: [borkarvp@gmail.com](mailto:borkarvp@gmail.com)

[a\*] Dhempe college of Arts and Science, Panaji Goa, 403001, India.

[b] Department of Chemistry, Government College of Arts, Science and Commerce, Khandola, Goa, 403107, India

[c] Rani Chennamma University, Belgaum 591156, India

The pollution in mining area is mainly because of ore reject: material remaining after beneficiation of the ore. These rejects/tailings are generally stored in the pits developed during mining. During rains they flow in the fields and ruin crops. They contain more than 40 % Fe which is wasted. We used iron ore reject for degradation of model organic dye methylene blue (MB) giving rejects a value addition.<sup>21</sup>

## Introduction

The dyes present in textile effluent pollute the water bodies. Materials like agricultural waste, ash, oxides of zinc, titania, iron<sup>1-9</sup> etc. are used in waste treatment of industrial effluent. The oxides are also used in degradation of hazardous gases, removal of organic pollutants and inhibition of undesirable microorganisms from water.<sup>10</sup> Zinc and titanium oxides are used as photocatalyst in organic dye degradation using UV radiation of ~378 nm. Zinc oxide is a semiconductor with an average bandgap of 3.37 eV and has varied applications.<sup>11</sup> It generates electron-hole pairs on exposure to ultraviolet radiations. However, sunlight consists ~2 % UV, limits the use of solar radiation for the photodegradation. Cation/anion doping of oxides is tried to enhance the photocatalytic properties.<sup>12</sup> Increased photocatalytic activity under visible light is mostly due to the synergistic effect of substantial nitrogen doping, high surface area and presence of oxygen vacancy in oxides.<sup>13</sup> Zinc oxide when doped with nitrogen replaces oxygen from the lattice forming ZnO<sub>1-x</sub>N<sub>x</sub> (x ≤ 0.15).<sup>14</sup> Decomposition of hydrazinated zinc oxalate forms yellow ZnO<sub>1-x</sub>N<sub>x</sub> (absorbs in the visible region of the sunlight).<sup>15</sup> Hydrazine modified precursors yield spinels, perovskites with large surface area.<sup>15-19</sup> ZnO<sub>1-x</sub>N<sub>x</sub> obtained from hydrazinated oxalate has surface area ~11.8 m<sup>2</sup>g<sup>-1</sup> and found to be good bactericidal agent effective against *E. coli* in our earlier work.<sup>20</sup> In the present investigation it is used for dye degradation.

Methylene blue (MB belongs to thiazine class of dyes) is difficult to decompose under visible light and is chosen as a model dye to evaluate photocatalysis.

Present study aims at comparison of MB degradation results using iron ore, zinc oxide and N doped zinc oxide. So oxalate and hydrazinated oxalate of zinc are synthesized, analysed and decomposed to yield ZnO and ZnO<sub>1-x</sub>N<sub>x</sub>. These oxides as well as iron ore reject are characterized and their efficacy is tested by photo-catalytic degradation of MB. Photodegradation products generated during investigation are compared to understand the relative efficacy of three photocatalysts.

## Experimental

### Synthesis of zinc oxide precursor

Zinc oxalate is prepared by the addition of aq. ammonium oxalate solution (0.5M, 100 mL) to an aq. zinc chloride solution (0.5M, 100mL). The precipitate of zinc oxalate is filtered and dried. Hydrazination of oxalate is done by keeping the dried zinc oxalate over hydrazine hydrate (Merck, 99 %) in a dessicator. The hydrazine uptake is monitored by KIO<sub>3</sub> titration.<sup>22</sup>

### Characterization of precursors and oxides

Standard chemical analysis, Infrared analysis (Shimadzu IR Prestige 21), TG/DTA studies (STA 409 PC LUXNETZCH) and isothermal weight loss study are carried out to fix formula for the zinc oxalate and its hydrazinated precursor. The decomposition temperature of both the precursors are obtained by TG/DTA recorded from room temperature to 1000 °C (heating rate-10K/min). The precursors are decomposed at ~700 °C to obtain zinc oxides.

Phase identification of the metal oxide is carried out by X-ray diffraction (Rigaku Powder X-ray diffractometer using  $\text{CuK}\alpha$  radiation,  $\lambda=1.5418 \text{ \AA}$ ). Scanning electron micrographs (SEM) of oxides are obtained on JEOL JSM – 5800.

Nitrogen analysis is made on HIROBA EMGA 2800. The diffuse reflectance spectra (DRS) of oxides are recorded on UV-2401-Rev A 6700 with diffuse reflectance accessory to determine the absorption in the range of 200-800 nm.  $\text{BaSO}_4$  is used as reference. The bandgap energies are calculated using equation: Band gap ( $E_g$ ) in eV =  $1239.8/\lambda_{\text{max}}$ . ( $\lambda_{\text{max}}$  is maximum wavelength of absorption from differential plots of reflectance spectra).

X ray photoelectron spectra, XPS is obtained at 298 K using  $\text{MgK}\alpha$  radiation on a VG Microtech Multilab ESCA 3000 spectrometer.

### Characterization of iron ore reject

The various studies carried out of iron ore reject such as chemical analysis by standard methods,<sup>22</sup> infrared analysis by Shimadzu IR Prestige 21, elemental analysis by EDS, diffuse reflectance spectrum (DRS) by UV-visible spectrophotometer (Shimadzu UV-2401-Rev A 6700) and saturation magnetization measurement by Satmagan (Saturation Magnetization Analyser) Model 135 of Corriagan make. The phase identification of the metal oxides present in reject is carried out by X-ray diffraction (Rigaku Powder X-ray diffractometer) and Scanning electron micrographs (SEM) by JEOL JSM – 5800.

### Photodegradation studies

Photodegradation or decolorization of an aqueous solution of methylene blue (MB), was monitored spectrophotometrically (Shimadzu UV-2401-Rev A 6700) at  $\lambda_{\text{max}} = 665 \text{ nm}$ . The solution of MB was maintained at neutral pH. 50 mL aqueous solution of MB dye ( $0.5 \times 10^{-4} \text{ M}$ ) with 200 mg of catalyst (ZnO or  $\text{ZnO}_{1-x}\text{N}_x$  or iron ore reject) added was exposed to sunlight. 2 mL of test solution was filtered after every 30 minutes of sunlight exposure and tested on spectrophotometer. Simultaneously solution of MB, without the catalyst was also exposed to sunlight and checked on spectrophotometer after every 30 minutes (to check photolysis). Solar light intensity and the power generated were measured every 30 minutes using Luxmeter LX-101 and solar kit of TATA BP Solar Bangalore, India respectively. The average light intensity during the experiment was 300 to 724 lux units. The power was 0.24  $\text{W cm}^{-1}$  to 0.52  $\text{W cm}^{-1}$ .

### Chemical and ESI-MS studies of the photodegradation products of methylene blue

The chemical oxygen demand (COD) test allows measurement of organic waste in water in terms of the total quantity of oxygen required for the oxidation of organic matter to  $\text{CO}_2$  and water.

COD of MB solution during degradation is measured by the standard  $\text{K}_2\text{Cr}_2\text{O}_7$  method.<sup>23</sup> The percentage of MB degraded or chemical oxygen demand removal ( $\phi$ , %) is calculated according to the equation,

$$\phi = 100 \frac{C_0 - C}{C_0}$$

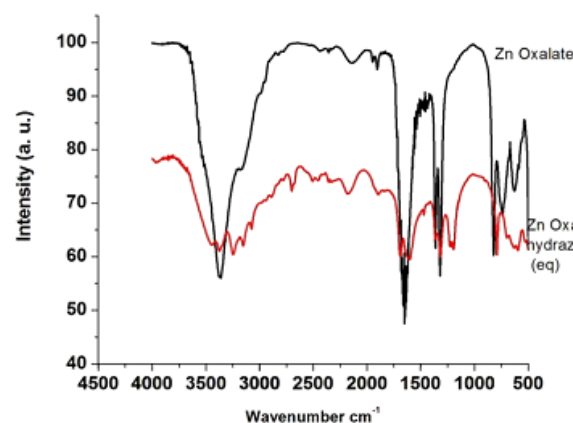
$C_0$  is the initial chemical oxygen demand ( $\text{mg L}^{-1}$ ) and  $C$  is the chemical oxygen demand after treatment ( $\text{mg L}^{-1}$ ).

The concentrations of nitrate ions,  $\text{NO}_3^-$ , sulfate ions,  $\text{SO}_4^{2-}$  and free  $\text{CO}_2$  ( $\text{mg L}^{-1}$ ) are tested after complete decolorization of MB by standard chemical methods.<sup>24, 25</sup> The decolorized solution is extracted with chloroform and the residue obtained after drying is dissolved in methanol and products are analyzed by electrospray ionization mass ESI-MS using an electrospray/quadrupole/time-of-flight (QTOF) mass spectrometer (QstarXL, MDS Sciex).

Zinc oxides and iron ore rejects are washed and dried after use and then reused for degradation. The reusability is tested three times.

## Results and discussion

We confirm formation of zinc oxalate and hydrazinated zinc oxalate from infra red studies (Fig.1) of precursors. The band positions are observed at 1300, 1654  $\text{cm}^{-1}$  due to  $\nu_s$  (o-c-o) and  $\nu_{\text{as}}$  (o-c-o) respectively. A broad band between 3000 to 3600  $\text{cm}^{-1}$  is due to  $\nu$  (OH).<sup>26-28</sup> Hydrazine linkage is developed with band position between 1130-1200  $\text{cm}^{-1}$  due to  $\delta$  ( $\text{NH}_2$ ) and between 3100-3500  $\text{cm}^{-1}$  due to  $\nu$ (N-H) stretching in hydrazinated zinc oxalate.

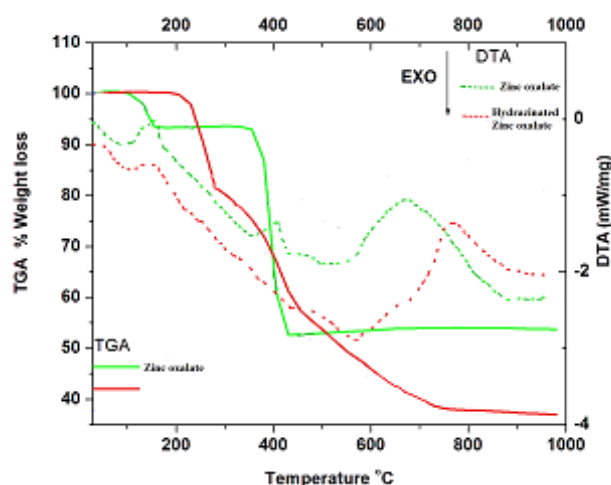


**Figure 1.** FTIR spectra of zinc oxalate and hydrazinated zinc oxalate

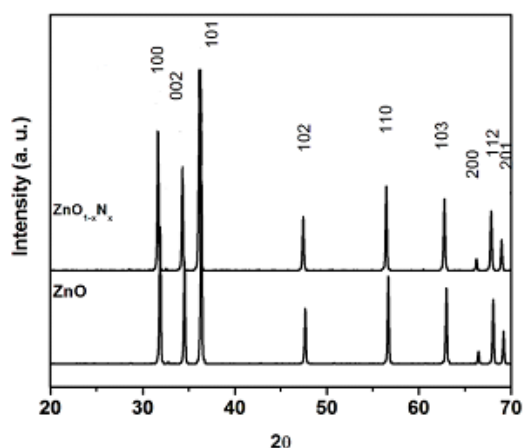
**Table 1.** Hydrazine content, oxalate content and weight loss study of precursors

Precursor	Hydrazine content, %		Oxalate content, %		Total Weight loss %		
	Calculated	Observed	Calculated	Observed	Calculated	TG	Isothermal
ZnC <sub>2</sub> O <sub>4</sub> ·2H <sub>2</sub> O	-	-	46.4	46.2	57.0	60.5	57.03
ZnC <sub>2</sub> O <sub>4</sub> ·N <sub>2</sub> H <sub>4</sub> ·H <sub>2</sub> O	15.7	15.5	43.2	44.0	59.9	61.3	59.60

TG (Fig. 2) showed major weight loss of ~60 % till 600 °C in both precursors. The endotherms and exotherms till 600 °C in DTA suggested that dehydration, decarboxylation, dehydrazination and decomposition occurs till this temperature. A small endotherm at ~678 °C in zinc oxalate and ~759.4 °C in hydrazinated complex is due to structure formation (no weight loss occurs in TG at these temperatures).

**Figure 2.** TG/DTA of zinc oxalate and hydrazinated zinc oxalate

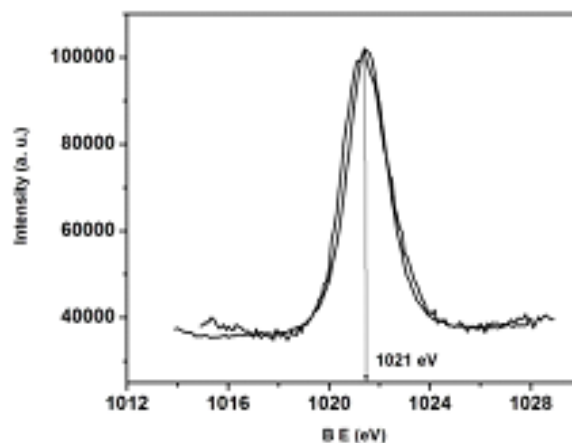
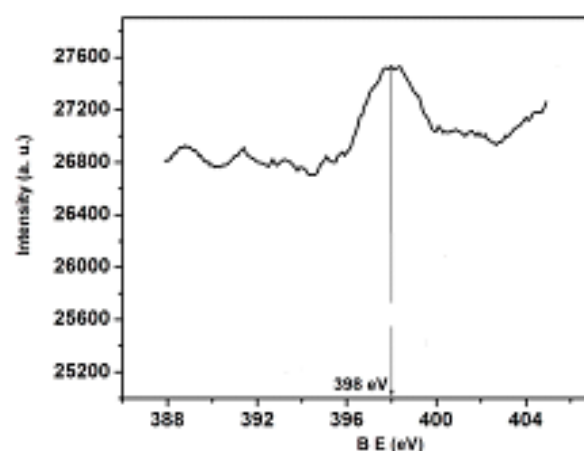
Total weight loss study, TG/DTA study and chemical analysis (hydrazine and oxalate content) of complex confirmed formula of zinc oxalate as ZnC<sub>2</sub>O<sub>4</sub>·2H<sub>2</sub>O and hydrazinated complex as ZnC<sub>2</sub>O<sub>4</sub>·N<sub>2</sub>H<sub>4</sub>·H<sub>2</sub>O (Table 1).

**Figure 3.** XRD of ZnO and ZnO<sub>1-x</sub>N<sub>x</sub>

The complexes were decomposed at 700°C; the former yielded white oxide and the later yellow. XRD of decomposed complexes, Fig. 3 match well with the Joint Committee on Powder Diffraction Standards (JCPDS) file of

ZnO (Wurtzite). 13.75 % Nitrogen was present in ZnO<sub>1-x</sub>N<sub>x</sub> (yellow), measured by oxygen and nitrogen analyzer. However there was no difference in XRD pattern of ZnO and ZnO<sub>1-x</sub>N<sub>x</sub>. Similar observations were reported.<sup>14</sup>

XPS studies of ZnO<sub>1-x</sub>N<sub>x</sub> were recorded for N1s and Zn2p<sub>3/2</sub> core levels. The N1s core level appeared at a binding energy (B.E.) ~ 398 eV Fig. 4.

**Figure 4.** X-ray photoelectron spectrum of (a) N 1s and (b) Zn 2p electron in ZnO<sub>1-x</sub>N<sub>x</sub>

This suggests N in ZnO<sub>1-x</sub>N<sub>x</sub> is similar to NH<sub>3</sub> or amines. The nitride B.E. is reported to be ~397 eV. So electron density on nitrogen is less than that of nitrides. Zn 2p core level shows B. E. ~ 1021 eV (Fig.4b). The lower B.E. of Zn 2p core level (reported, 1022 eV<sup>14</sup>) is due to covalent nature of Zn-N bond. These observations were similar to reported.<sup>14</sup> They suggest that electron density on Zn in ZnO<sub>1-x</sub>N<sub>x</sub> is slightly more than ZnO. Nitrogen donated some electrons to Zn. This enhanced photocatalytic degradation of MB.

Diffuse reflectance spectra (Fig. 5) of ZnO and ZnO<sub>1-x</sub>N<sub>x</sub> showed that the former absorbed in UV region and later in the visible region; indicating the possibility of photocatalysis by ZnO<sub>1-x</sub>N<sub>x</sub> with visible light.

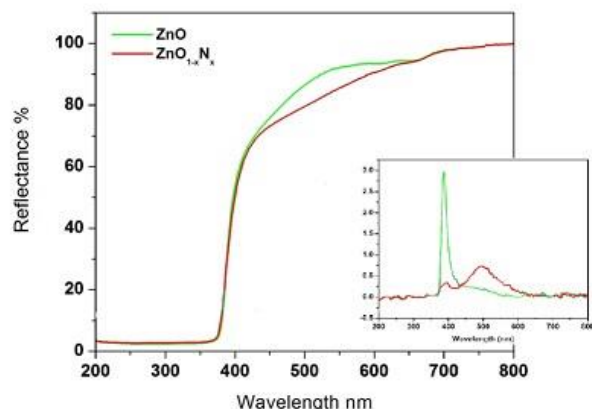


**Figure 5.** Diffuse reflectance spectra of ZnO and ZnO<sub>1-x</sub>N<sub>x</sub> (inset derivative of the diffuse reflectance spectra)

The band gap energy calculated from derivative of the spectra is 3.19 eV for ZnO and 2.48 eV for ZnO<sub>1-x</sub>N<sub>x</sub>. The lower value of energy of ZnO<sub>1-x</sub>N<sub>x</sub> helped in increasing number of electron hole pair thus enhancing the dye degradation. Scanning electron micrographic studies (Fig. 6) of ZnO<sub>1-x</sub>N<sub>x</sub> indicated uniform particles ~69 nm and ZnO, ~0.5-2 μm with BET surface area of ~ 11.8 m<sup>2</sup>g<sup>-1</sup> and 8.137 m<sup>2</sup>g<sup>-1</sup> respectively. The large surface area of ZnO<sub>1-x</sub>N<sub>x</sub>, and less band gap energy (electrons excitation better) are important parameters in photocatalysis.

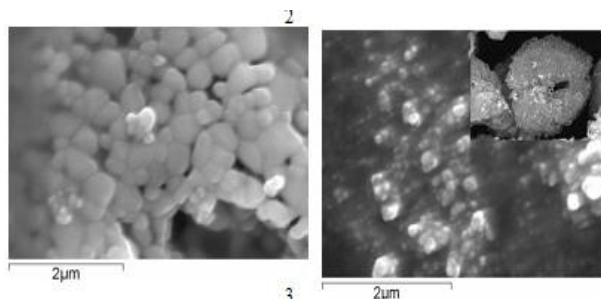


**Figure 6.** SEM pictures (a) ZnO (b) ZnO<sub>1-x</sub>N<sub>x</sub>

Chemical analysis of ore reject revealed the presence of 54% total Fe reported in earlier work<sup>21</sup>. XRD analysis of iron ore rejects Fig. 7 and EDS results<sup>21</sup> (Table 2) showed the presence of Fe<sub>2</sub>O<sub>3</sub> (α, γ, ε), Fe<sub>3</sub>O<sub>4</sub>, α-FeOOH, SiO<sub>2</sub>, Al<sub>2</sub>O<sub>3</sub> and small amounts of MnO<sub>2</sub>. The peak positions were matched with the JCPDS files.

**Table 2.** EDS results of analysis on iron ore reject

Element	Weight%	Atomic%
O K	43.64	71.07
Al K	2.74	2.64
Si K	2.60	2.42
K K	0.32	0.21
Mn K	0.70	0.33
Fe K	50.00	23.33

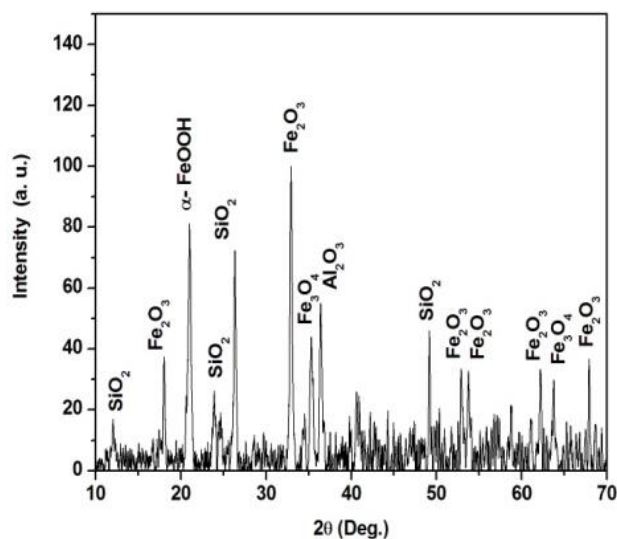


**Figure 7.** XRD of iron ore reject

FTIR of ore reject Fig. 8, showed absorption at 545 cm<sup>-1</sup> due to Fe-O in Fe<sub>3</sub>O<sub>4</sub>.

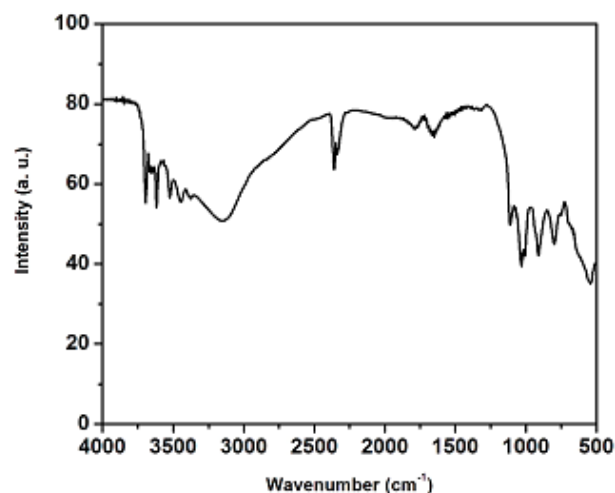


**Figure 8.** FT-IR of iron ore reject

The presence of broad and intense absorption band at 3100-3200 cm<sup>-1</sup> was due to FeOOH, at 795, 913 cm<sup>-1</sup> due to O-H bending, 1650 cm<sup>-1</sup> due to H-O-H bending and at 3694 cm<sup>-1</sup> due to surface hydroxyl groups. These results agreed well with results of XRD and EDS.

Iron ore reject showed different sizes and shapes of particles Fig. 9.

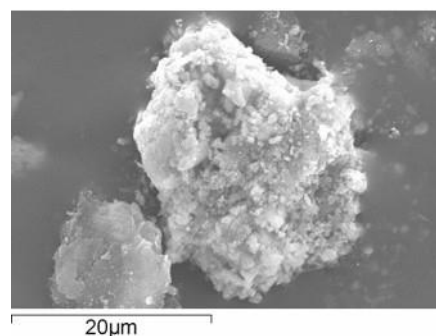


**Figure 9.** SEM picture of iron ore reject

Diffuse reflectance spectra (Fig.10) of iron ore reject revealed the absorption in visible region.

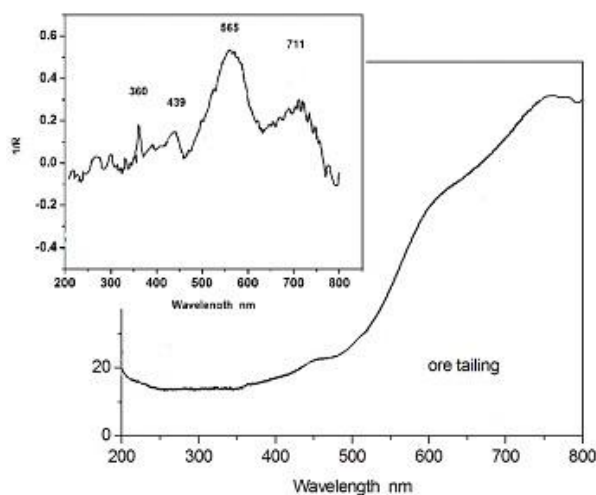


**Figure 10.** Diffuse reflectance spectra of iron ore reject (inset derivative of the diffuse reflectance spectra)

The band gap energy calculated was 2.39 eV. The derivative peaks may be assigned to the phases Goethite ( $\alpha$ -FeOOH) at 439 nm, Maghemite ( $\gamma$ -Fe<sub>2</sub>O<sub>3</sub>) at 360 nm, Hematite ( $\alpha$ -Fe<sub>2</sub>O<sub>3</sub>) at 565 nm and Magnetite (Fe<sub>3</sub>O<sub>4</sub>) at 711 nm.<sup>29-31</sup> Components present in reject absorb in visible region enhancing the photo catalysis in sunlight.

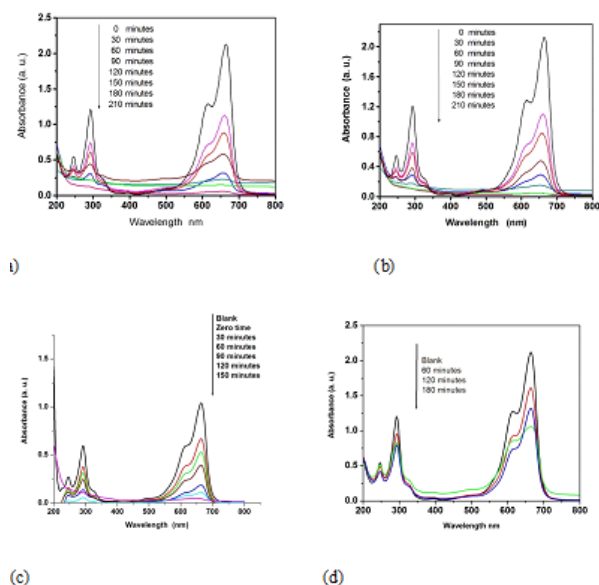


**Figure 11.** UV-Visible spectra of MB (pH=7) during degradation using a) ZnO; b) ZnO<sub>1-x</sub>N<sub>x</sub>; c) iron ore rejects; d) photolysis(absence of catalyst)

Maxima of UV-Visible absorbance spectra of methylene blue ( $\lambda_{max}=665$  nm) diminished with increase in sunlight exposure time in presence of ZnO, ZnO<sub>1-x</sub>N<sub>x</sub> and iron ore reject (Fig. 11a, b, c) due to breaking of the dye molecule. In presence of sunlight and ZnO (white) MB showed decolorisation in 210 minutes, in presence of ZnO<sub>1-x</sub>N<sub>x</sub> (yellow) in 210 minutes, and in presence of iron ore reject in 150 minutes. Only sunlight exposure (photolysis-without addition photocatalyst), showed decrease in absorbance

maxima but required 1200 minutes for decolorisation. The plot (Fig. 12) of variation in Absorbance of MB solution with time of sunlight exposure in presence of ZnO<sub>1-x</sub>N<sub>x</sub> and iron ore reject showed a sharp decrease. Photolysis (absence of any catalyst) degraded MB marginally.

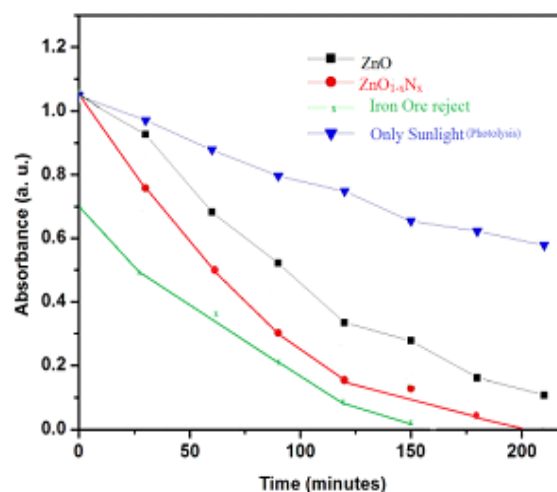


**Figure 12.** Decrease in absorbance of  $0.5 \times 10^{-4}$  M MB solution with sunlight exposure (the average light intensity, 300 to 724 lux units and the power, 0.24 to  $0.52 \text{ W cm}^{-2}$ ).

The kinetic study of MB degradation in sunlight using photocatalysts revealed that it follows first order equation:

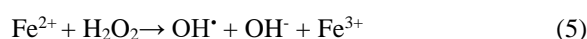
$$kt = \ln \frac{C_0}{C}$$

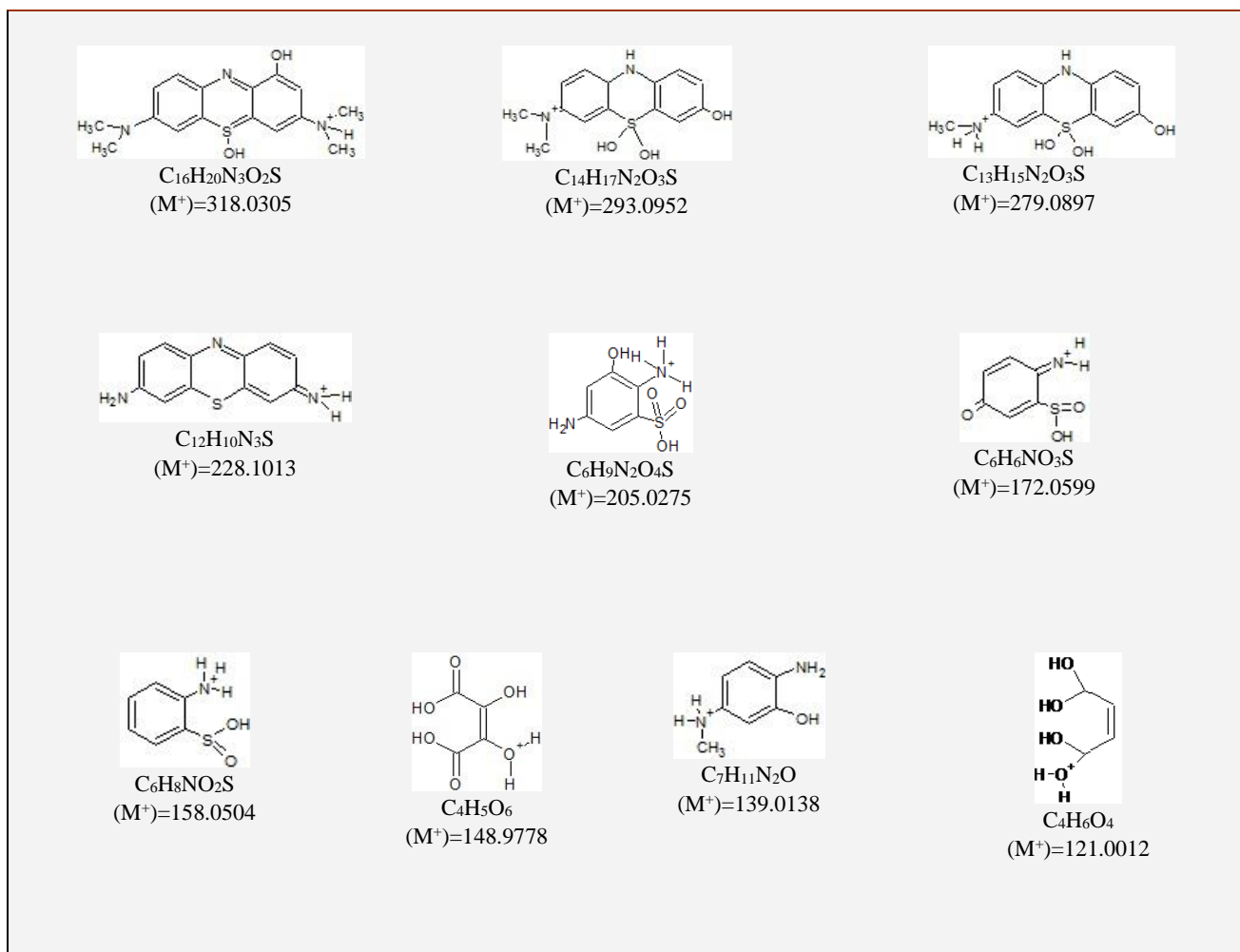
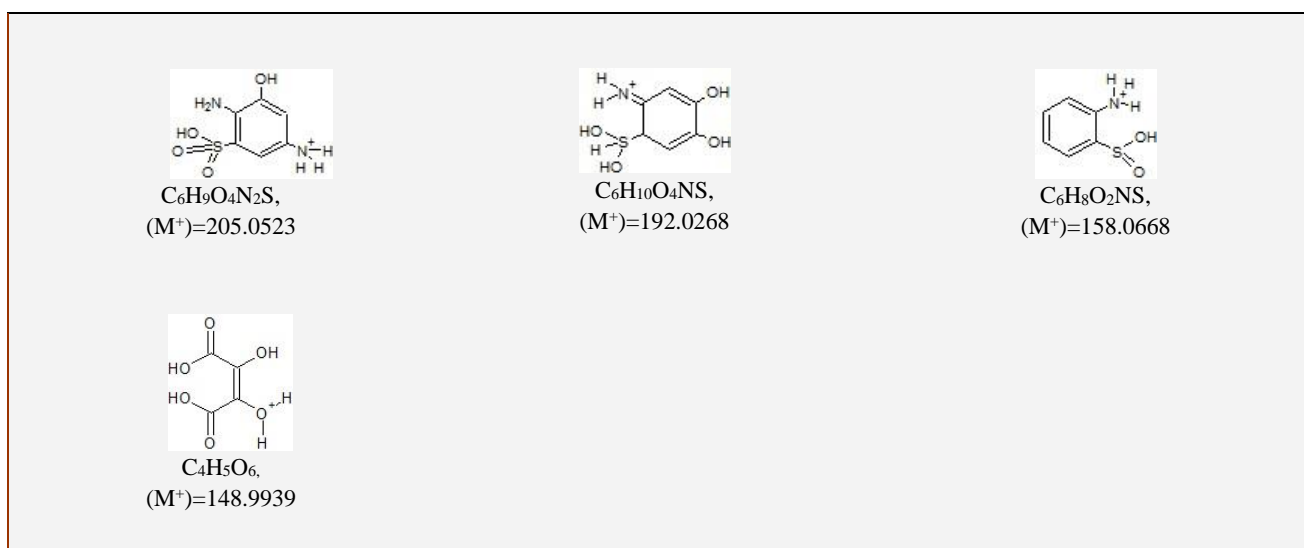
where  $k$  is rate constant. The rate constants were listed in Table 3.

**Table 3.** Percent degradation and the rate constants for MB degradation

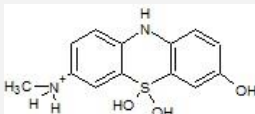
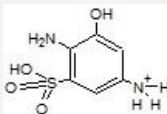
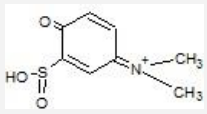
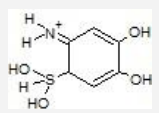
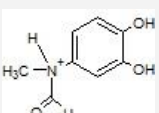
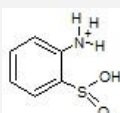
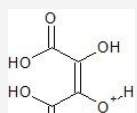
Photocatalyst	% degradation for $0.5 \times 10^{-4}$ M MB	$k, \text{min}^{-1}$
ZnO	90%	$8.36 \times 10^{-3}$
ZnO <sub>1-x</sub> N <sub>x</sub>	98%	$14.7 \times 10^{-3}$
Iron ore reject	97%	$17.3 \times 10^{-3}$
Photolysis	45%	$3.11 \times 10^{-3}$

The rate constant values indicated efficiency of ZnO<sub>1-x</sub>N<sub>x</sub> ( $14.7 \times 10^{-3} \text{ min}^{-1}$ ) compared to the ZnO ( $8.36 \times 10^{-3} \text{ min}^{-1}$ ) in dye degradation. The rate constant,  $k$  was highest for iron ore reject degradation,  $17.3 \times 10^{-3} \text{ min}^{-1}$ . Degradation by ore rejects<sup>21</sup> is due to formation of H<sub>2</sub>O<sub>2</sub> by Fe<sup>2+</sup>/Fe<sup>3+</sup> similar to explanation by Fenton.<sup>32</sup>

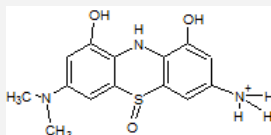
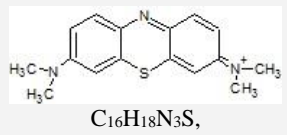
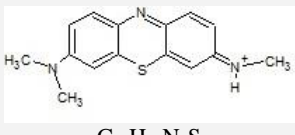
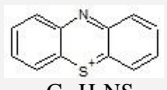
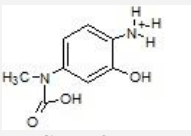
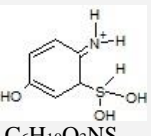
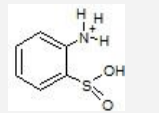
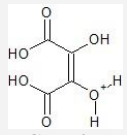


**Table 4.** Products of MB degradation on iron ore reject photocatalyst analyzed by ESI-MS.**Table 5.** Products of MB degradation using ZnO<sub>1-x</sub>N<sub>x</sub> analyzed by ESI-MS.

**Table 6.** Products of MB degradation on ZnO photocatalyst analyzed by ESI-MS.

			
C <sub>13</sub> H <sub>15</sub> O <sub>3</sub> N <sub>2</sub> S, (M <sup>+</sup> )=279.1189	C <sub>6</sub> H <sub>9</sub> O <sub>4</sub> N <sub>2</sub> S, (M <sup>+</sup> )=205.0545	C <sub>8</sub> H <sub>10</sub> O <sub>3</sub> NS, (M <sup>+</sup> )=200.0814	
			
C <sub>6</sub> H <sub>10</sub> O <sub>4</sub> NS, (M <sup>+</sup> )=192.0265	C <sub>8</sub> H <sub>10</sub> O <sub>3</sub> N, (M <sup>+</sup> )=167.9653	C <sub>6</sub> H <sub>8</sub> O <sub>2</sub> NS, (M <sup>+</sup> )=158.0668	C <sub>4</sub> H <sub>5</sub> O <sub>6</sub> , (M <sup>+</sup> )=148.9934

**Table 7.** Products of solar degradation of MB without catalyst (photolysis) analyzed by ESI-MS.

		
C <sub>14</sub> H <sub>16</sub> O <sub>3</sub> N <sub>3</sub> S, (M <sup>+</sup> )=306.1127	C <sub>16</sub> H <sub>18</sub> N <sub>3</sub> S, (M <sup>+</sup> )=284.07774	C <sub>15</sub> H <sub>16</sub> N <sub>3</sub> S, (M <sup>+</sup> )=270.0679
		
C <sub>12</sub> H <sub>8</sub> NS, (M <sup>+</sup> )=198.0964	C <sub>8</sub> H <sub>11</sub> O <sub>3</sub> N <sub>2</sub> , (M <sup>+</sup> )=183.0843	C <sub>6</sub> H <sub>10</sub> O <sub>3</sub> NS, (M <sup>+</sup> )=176.1126
		
C <sub>6</sub> H <sub>8</sub> O <sub>2</sub> NS, (M <sup>+</sup> )=158.0690	C <sub>4</sub> H <sub>5</sub> O <sub>6</sub> , (M <sup>+</sup> )=148.9956	

Oxygen adsorbed on surface of iron ore reject takes electron from the substrate and forms oxygen radical, which later reacts with water molecule forming hydrogen peroxide. Fe<sup>2+</sup> of the ore gets oxidized by hydrogen peroxide to form Fe<sup>3+</sup>, a hydroxyl radical and a hydroxyl anion.

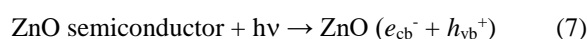


Another molecule of hydrogen peroxide converted Fe<sup>2+</sup> back to Fe<sup>3+</sup>, a peroxide radical and a proton. The hydroxyl radicals (OH<sup>•</sup>) are effective in destroying organic dye molecules. This chain reaction continuously generates hydroxyl radical at each conversion.

Continuous formation of Fe<sup>2+</sup> and Fe<sup>3+</sup> during MB degradation by iron ore is responsible for fast decolorisation in 150 minutes and highest *k* (17.3x10<sup>-3</sup> min<sup>-1</sup>). SATMAGAN study has confirmed increased amount of Fe<sup>2+</sup> after each use. Fe<sub>3</sub>O<sub>4</sub> content of reject was 5.02 %.

It increased to 5.55 % after first use. Fe<sub>3</sub>O<sub>4</sub> contains Fe<sup>2+</sup> so efficiency of ore rejects increases after each use.

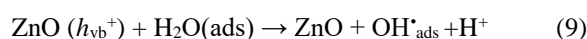
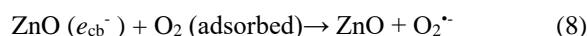
Following reactions are followed during degradation of MB by ZnO.<sup>33</sup>



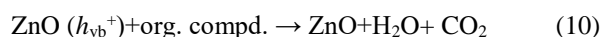
where

$e_{\text{cb}}^-$  = electrons in the conduction band (cb);

$h_{\text{vb}}^+$  = holes in the valence band (vb)



Direct oxidation of organic molecule by surface holes was also possible.



Using ESR spectroscopic data it is reported that the formation of active  $\text{OH}^{\cdot}$  and  $\text{O}_2^{\cdot-}$  species takes place during photodegradation of organic compounds.<sup>34</sup>

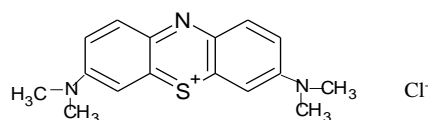


Thus hydroxyl radicals are formed during degradation of MB in presence of all three photocatalyst. More the number of electron hole pairs formed more will be formation of these radicals.  $\text{ZnO}_{1-x}\text{N}_x$  was yellow in colour due to loss of oxygen from lattice. Such non stoichiometric oxygen deficiencies lead to n-type semiconductor and absorb radiation in the visible region. Higher amount of visible radiations in sunlight compared to UV enhances electron pair formation when yellow  $\text{ZnO}_{1-x}\text{N}_x$  is used then white ZnO. XPS results also have inferred that nitrogen in the lattice donates electrons to Zn, so these electrons generate hydroxyl radicals. Increased formation of hydroxyl radical formation in  $\text{ZnO}_{1-x}\text{N}_x$  is responsible for higher value of rate constant  $k$  ( $14.7 \times 10^{-3} \text{ min}^{-1}$ ) compared to the ZnO ( $8.36 \times 10^{-3} \text{ min}^{-1}$ ). Reports<sup>14</sup> claim that  $\text{ZnO}_{1-x}\text{N}_x$  is effective in catalysis application as compared to ZnO and our study confirms the same.

However when iron ore reject is used there is continuous formation of hydroxyl radicals and so the degradation is faster than zinc oxides.

It is reported<sup>33</sup> that the  $\text{OH}^{\cdot}$  radicals attack the  $\text{C-S}^+=\text{C}$  functional group in MB ( $\text{C}_{16}\text{H}_{18}\text{N}_3\text{S}^+\text{Cl}^-$ ) forming sulfoxide ( $\text{RS(=O)R}'$ ) (equation 14). The attack of the second  $\text{OH}^{\cdot}$  radical on the sulfoxide produces sulfone ( $\text{RSO}_2\text{R}'$ ) (equation 15) and causes the dissociation of two benzenic rings. Sulfone then gives rise to sulfonic acid ( $\text{RSO}_3\text{H}$ ) (equation 17) which further gets oxidised to sulphate ion (equation 18).

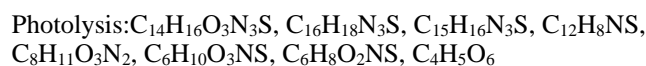
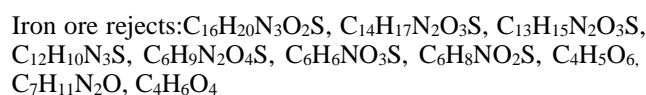
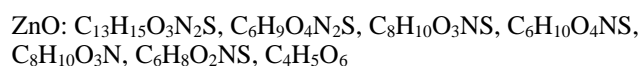
#### Methylene blue degradation



So degradation is directly proportional to hydroxyl radicals formed.

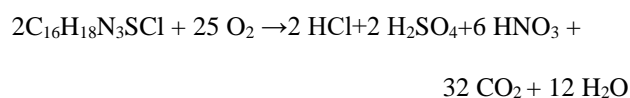
Detection of hydroxylated products in ESI-MS study (Table 4, 5, 6, and 7) confirmed that photodegradation of MB by three photocatalysts proceeded through hydroxyl radical mechanism.

The peak at  $m/z=284$  in photolysed MB (without catalyst) correspond to methylene blue molecular ion. The peak at  $m/z = 270$ , and 198 correspond to loss of methyl groups, and dimethyl amino groups from aromatic rings on both sides of MB respectively. The peaks at  $m/z = 306$ , 279 were due to successive addition of hydroxyl in the MB molecule. The breaking of MB molecule was suggested by the presence of peaks at  $m/z = 205$ , 200, 192, 183, 176, 168, 158 and 149. Thus ESI-MS indicated presence of some organic moieties in the decolorized solution of MB. A careful comparison the degradation products of MB using ZnO,  $\text{ZnO}_{1-x}\text{N}_x$ , iron ore reject, and photolysis is



It suggests that photolysis of MB,  $\text{C}_{16}\text{H}_{18}\text{N}_3\text{S}\text{Cl}$ , lead to organic moiety having  $\text{C}_{16}$ ,  $\text{C}_{15}$ ,  $\text{C}_{14}$  in them while  $\text{ZnO}_{1-x}\text{N}_x$  showed organic moieties having  $\text{C}_6$  and  $\text{C}_4$ , so better degradation. When iron ore and ZnO were used decolourised solution also contained some molecules with  $\text{C}_{16}$ ,  $\text{C}_{13}$ , etc.

Decolorisation of MB did not convey about total degradation to nontoxic molecules. MB,  $\text{C}_{16}\text{H}_{18}\text{N}_3\text{S}\text{Cl}$  is blue in colour and leuco MB, reduced form of MB is colorless. It can be converted back to MB. Thus it should be confirmed that decolourisation in our investigation was not formation of leuco MB. The complete mineralization of the molecule<sup>35</sup> may be written as follows:



Formation of  $\text{SO}_4^{2-}$ ,  $\text{NO}_3^-$  and  $\text{CO}_2$  from the degraded MB solution (Table 8) indicated the mineralization of the dye.

Concentration of free  $\text{CO}_2$  after 150 minutes was;  $14.25 \text{ mg L}^{-1}$  in presence of  $\text{ZnO}_{1-x}\text{N}_x$ ,  $10.69 \text{ mg L}^{-1}$  in presence of ZnO, and  $49.89 \text{ mg L}^{-1}$  in case of iron ore reject. Thus iron ore reject was able to convert more organic moiety into  $\text{CO}_2$ . % COD removal was highest when  $\text{ZnO}_{1-x}\text{N}_x$  (90 %) and iron ore reject (86 %) were used. Direct photolysis showed an increase in the COD from 84 % to 294 % after 30 minutes of light exposure. It further increased to ~572 % on complete decolourization (required ~ 20 h) revealing presence of organic moiety in solution after decolourisation.

Table 8. % COD, amount of free CO<sub>2</sub>, nitrate and sulphate generated during MB photo degradation in presence of catalyst

Catalyst added	COD mg L <sup>-1</sup>			% COD removal	Free CO <sub>2</sub> t <sub>150</sub>	Nitrate, mg L <sup>-1</sup> t <sub>150</sub>	Sulphate mg L <sup>-1</sup>	
	t <sub>0</sub>	t <sub>30</sub>	t <sub>150</sub>				t <sub>30</sub>	t <sub>150</sub>
Iron ore reject	84	44	12	86	49.89	0.77	2.55	3.10
ZnO <sub>1-x</sub> N <sub>x</sub>	84	36	08	90	14.25	0.80	0.11	0.90
ZnO	84	44	28	67	10.69	0.80	0.16	0.88
Photolysis (only sunlight)	84	294	572.4	COD added	-	2.60	0.75	32.5

Table 9. %COD, amount of free CO<sub>2</sub>, nitrate and sulphate generated during MB photo degradation when catalysts are reused

	ZnO			ZnO <sub>1-x</sub> N <sub>x</sub>			Iron ore reject		
	COD %	sulphate mg L <sup>-1</sup>	nitrate mg L <sup>-1</sup>	COD %	sulphate mg L <sup>-1</sup>	nitrate mg L <sup>-1</sup>	COD %	sulphate mg L <sup>-1</sup>	nitrate mg L <sup>-1</sup>
1 cycle	67	0.88	0.8	90.47	0.8	0.99	85.71	3.101	0.77
2 cycle	69.05	3.0	1.8	69.05	2.4	1.32	90	1.92	3.0
3 cycle	80.95	2.2	1.8	78.5	7.9	2.6	73.8	4.6	5.99

ESI-MS study (Table 7) supported this observation. The photolysis led to incomplete mineralization and formation of oxygen demanding organic species. ZnO with its wide band gap of ~3.19 eV effectively absorbed the UV radiation of the sunlight (~2 % UV in sunlight reaches earth crust) and produced the electron hole pair and initiated photodegradation. N-doped ZnO due to the band gap modification (~2.48 eV in DRS study) and absorption of visible light lead to increased electron hole production, enhancing photocatalysis, higher % COD removal and CO<sub>2</sub> formation. Electron-hole recombination also decreased due to the band gap modifications.

Lack of nitrate content in the early stages of degradation was due to formation of ammonium ions initially and later oxidation to nitrates. Quantity of sulphate ions released was low due to the formation of gases, H<sub>2</sub>S/SO<sub>2</sub>.<sup>31, 33</sup>

200 mg ZnO<sub>1-x</sub>N<sub>x</sub> was able to degrade 50 mL of 0.5x10<sup>-4</sup> M MB in 150 minutes with ~90 % COD removal, 0.8 mg L<sup>-1</sup> NO<sub>3</sub><sup>-</sup> and 0.99 mg L<sup>-1</sup> SO<sub>4</sub><sup>2-</sup>. It also showed reusability (Table 9) with increased formation of sulphates and nitrates. Time required for de-colorization of MB by ZnO<sub>1-x</sub>N<sub>x</sub> was constant during reuse but showed a decrease in COD removal in the 2<sup>nd</sup> run (Table 9).

200 mg of ore reject was able to degrade 50 mL of 0.5x10<sup>-4</sup> M MB in 150 minutes with ~86 % COD removal, 0.77 mg L<sup>-1</sup> NO<sub>3</sub><sup>-</sup> and 3.1 mg L<sup>-1</sup> SO<sub>4</sub><sup>2-</sup>. Thus ore had better mineralizing action as compared to ZnO and ZnO<sub>1-x</sub>N<sub>x</sub>. Degradation enhanced during its reuse due to conversion of Fe<sup>3+</sup> to Fe<sup>2+</sup> ions which increased formation of hydroxyl ions. The degradation time decreased from 150 minutes to 120 minutes and 90 minutes during the second and third use, respectively. ZnO<sub>1-x</sub>N<sub>x</sub> did not show this trend. 2 g of reject added to 50 mL of 0.5x10<sup>-4</sup> M MB was able to degrade the dye instantaneously. This was also not observed when 2 g ZnO<sub>1-x</sub>N<sub>x</sub> were used.

All catalysts were reused three times (Table 9) without losing the original activity suggesting that there was negligible adsorption of the degradation products on their surface.

## Conclusions

The two precursors zinc oxalate and hydrazinated zinc oxalate were synthesized. On decomposition, zinc oxalate yielded white ZnO and hydrazinated zinc oxalate yellow ZnO<sub>1-x</sub>N<sub>x</sub>. Presence of nitrogen in yellow oxide was confirmed by XPS and oxygen nitrogen analyser. N-doped zinc oxide, ZnO<sub>1-x</sub>N<sub>x</sub> obtained from the hydrazinated precursor required less time for degradation of the methylene blue dye as compared to ZnO. ESI-MS results indicate presence of small amounts of some organic moieties on complete decolourization. Photolysis of MB, C<sub>16</sub>H<sub>18</sub>N<sub>3</sub>SCl, lead to formation of organic moiety having C<sub>16</sub>, C<sub>15</sub>, C<sub>14</sub> in them while ZnO<sub>1-x</sub>N<sub>x</sub> lead to formation of molecules with C<sub>6</sub> and C<sub>4</sub>. No loss in the efficiency of ZnO and ZnO<sub>1-x</sub>N<sub>x</sub> makes them suitable for reuse. The electron-hole pair formation in ZnO and ZnO<sub>1-x</sub>N<sub>x</sub> on exposure to sunlight lead to hydroxyl radical formation, those are responsible for degradation. ZnO<sub>1-x</sub>N<sub>x</sub> absorbs in visible region and so more electron hole pairs are formed. In XPS study it is inferred that nitrogen is likely to donate some electrons to Zn. So they also enhance generation of hydroxyl radicals. This increases efficiency of ZnO<sub>1-x</sub>N<sub>x</sub>. Band gap energy calculated from DRS are 2.48 eV and 3.19 eV for ZnO<sub>1-x</sub>N<sub>x</sub> and ZnO respectively indicating easier electron excitation in the former than later. Thus ZnO<sub>1-x</sub>N<sub>x</sub> showed better dye degradation. Iron ore reject contained about 54 % total Fe with lower band gap energy 2.39 eV. The time required for dye degradation using iron ore rejects is least, 150 minutes with higher first order rate constant 17.3x10<sup>-3</sup> min<sup>-1</sup> as compared to ZnO which required 210 minutes with *k*, 8.36x10<sup>-3</sup> min<sup>-1</sup> and ZnO<sub>1-x</sub>N<sub>x</sub> with *k*, 14.7x10<sup>-3</sup> min<sup>-1</sup>. During degradation ore reject forms hydroxyl ion radicals similar to fenton reagent. Chain reaction during the process supplies hydroxyl ions continuously due to formation of Fe<sup>3+</sup>/Fe<sup>2+</sup>. Hence efficacy of ore reject is best amongst the three. Increased amount of Fe<sup>2+</sup> during reuse is proved by SATMAGAN. The dye molecule is converted to gases. Formation of SO<sub>4</sub><sup>2-</sup>, NO<sub>3</sub><sup>-</sup> and CO<sub>2</sub> indicated the mineralization of the dye. Concentration of SO<sub>4</sub><sup>2-</sup> and free CO<sub>2</sub> is found higher when ore reject is used for degradation. % COD removal is higher for iron ore reject and ZnO<sub>1-x</sub>N<sub>x</sub>.

Thus Iron ore rejects, an environmental pollutant, easily available on mining sites can be used to degrade dyes and other unsaturated organic compounds then synthesizing oxides. Comparing the three photocatalysts for dye degradation, iron ore reject  $> \text{ZnO}_{1-x}\text{N}_x > \text{ZnO}$ .

## Acknowledgement

Authors thank Dr. C. G. Naik, National Institute of Oceanography, Goa, India for helping in ESI-MS study and Dr. Gopinath S. C., National Chemical Laboratories, Pune, India for XPS study.

## References

- <sup>1</sup>Smelcerovic M., Dordevic D., Novakovic M., Mizdrakovic M., *J. Serbian Chem. Soc.*, **2010**, 75(6), 855.
- <sup>2</sup>Sriwong C., Wongnawa S., Patarapaiboolchai O., *J. Environ. Sci.*, **2012**, 24, 464.
- <sup>3</sup>Elghniji K., Hentati O., Mlaik N., Mahfoudh A., Ksibi M., *J. Environ. Sci.*, **2012**, 24, 479.
- <sup>4</sup>Rashed M. N., El-amin A.A., *Intern. J. Phys. Sci.*, **2007**, 2, 73.
- <sup>5</sup>Noorjahan M., Pratap Reddy M., Durga Kumari, V., Lavedrine, B., Boule, P., Subrahmanyam, M., *J. Photochem. Photobiol. A: Chem.*, **2003**, 156, 179.
- <sup>6</sup>Chakrabarti, S., Dutta B. K., *J. Hazard. Mater.*, **2004**, 112, 433.
- <sup>7</sup>Byrappa K., Subramani, A. K., Ananda, S., Lokanatha Rai, K. M. and Dinesh, R., *Bull. Mater. Sci.*, **2006**, 29, 433.
- <sup>8</sup>Daneshvar N., Aber S., Seyed Dorraji M. S., Khataee A. R. and Rasoulifard M. H., *Int. J. Chem. Biomol. Eng.*, **2008**, 1, 24.
- <sup>9</sup>Liu, H., Yang, Y., Kang, J., Fan, M., Qu, J., *J. Environ. Sci.*, **2012**, 24, 242.
- <sup>10</sup>Padmavathy, N., Vijayaraghavan, R., *Sci. Techn. Adv. Mater.*, **2008**, 9, 1.
- <sup>11</sup>Moezzi, A., McDonagh, A. M., Cortie, M. B., *Chem. Eng. J.*, **2012**, 185, 1.
- <sup>12</sup>Rane, K. S., Mhalsiker, R., Yin, S., Sato, T., Cho, K., Dunbar E. and Biswas, P., *J. Solid State Chem.*, **2006**, 179, 3033.
- <sup>13</sup>Noor, A., Mishra, T., Sahu, R. K. and Tiwari, J. P., *J. Mater. Chem.*, **2010**, 20, 10876.
- <sup>14</sup>Mapa, M. and Gopinath, C. S., *Chem. Mater.*, **2009**, 21, 351.
- <sup>15</sup>Rane, K. S., Uskaikar, H., Pednekar, R. and Mhalsikar, R., *J. Therm. Anal. Calor.*, **2007**, 90, 627.
- <sup>16</sup>Moye, V., Rane, K. S. and Kamat Dalal, V. N., *J. Mater. Sci. Mater. Electr.*, **1990**, 1, 212.
- <sup>17</sup>Borker, V., Rane, K. S., Kamat Dalal, V. N., *J. Mater. Sci. Mater. Electr.*, **1993**, 4, 241.
- <sup>18</sup>Rane, K. S., Verenkar, V. M. S. and Sawant, P. Y., *Bull. Mater. Sci.*, **2001**, 24, 323.
- <sup>19</sup>Rane, K. S., Verenkar, V. M. S. and Sawant, P. Y., *Bull. Mater. Sci.*, **2001**, 24, 331.
- <sup>20</sup>Karmali, R. S., Bartakke, A., Borker, V. P., Rane, K. S., *Biointerface Res. Appl. Chem.*, **2011**, 1, 57.
- <sup>21</sup>Karmali, R. S., Borker, V. P., Rane, K. S., Naik, C. G., *J. Solid Waste Manag.*, **2012**, 38, 232.
- <sup>22</sup>Vogel I. A., “*Textbook of Quantitative Inorganic analysis*”, Longman, UK., **1978**.
- <sup>23</sup>Feng, X., Zhu, S., Hou, H., *Water S. A.*, **2006**, 32, 43.
- <sup>24</sup>Manivasakam, N., *Physicochemical examination of water sewage and industrial effluents*, Pragati Prakashan, Meerut, **1980**.
- <sup>25</sup>Ramesh, R. and Anbu, M., *Chemical methods for environmental analysis, water and sediment*, Macmillan India Press, **1996**.
- <sup>26</sup>Fujita, J., Martell, A. E., Nakamoto, K., *J. hem, Phys.*, **1962**, 36, 324.
- <sup>27</sup>Fujita, J., Martell, A. E., Nakamoto, K., *J. Chem, Phys.*, **1962**, 36, 331.
- <sup>28</sup>Braibanti, A., Dallavalle, F., Pellinghelli, M. A., Leporati, E., *Inorg. Chem.*, 1968, 7, 1430.
- <sup>29</sup>Scheinost, A. C., Chavernas, A., Barron, V., Torrent, J., *Clays Clay Minerals*, **1998**, 46, 528.
- <sup>30</sup>Shen, Z. X., Cao, J. J., Zhang, X. Y., Arimoto, R., Ji, J. F., Balsam, W. L., Wang, Y. Q., Zhang, R. J., Li, X. X., *Sci. Total Environ.*, **2006**, 367, 899.
- <sup>31</sup>Cornell, R. M., Schwertmann, U., *The iron oxides: structure, properties, reactions, occurrences and uses*, 2<sup>nd</sup> Edition, Wiley-VCH, 2003.
- <sup>32</sup>Fenton, H. J. H., *J. Chem. Soc. Trans.*, **1894**, 65, 899.
- <sup>33</sup>Houas, A., Lachheb, H., Ksibi, M., Elaloui, E., Guillard, C., Herrmann, J., *Appl. Catal, B: Environ.*, **2001**, 31, 145.
- <sup>34</sup>Fu, H., Zhang, L., Zhang, S., Zhu, Y. and Zhao, J., *J. Phys. Chem. B*, **2006**, 110, 3061.
- <sup>35</sup>Nath, S., Ghosh, S. K., Panigrahi, S., Thundat, T., Pal, T., *Langmuir*, **2004**, 20, 7880.

Received: 17.03.2014.

Accepted: 15.04.2014.